

This article was downloaded by:

On: 14 January 2011

Access details: *Access Details: Free Access*

Publisher *Taylor & Francis*

Informa Ltd Registered in England and Wales Registered Number: 1072954 Registered office: Mortimer House, 37-41 Mortimer Street, London W1T 3JH, UK



## Molecular Simulation

Publication details, including instructions for authors and subscription information:

<http://www.informaworld.com/smpp/title~content=t713644482>

### Simulation of Chain-length Partitioning in a Microfabricated Channel via Entropic Trapping

Zhong Chen<sup>a</sup>; Fernando A. Escobedo<sup>a</sup>

<sup>a</sup> School of Chemical Engineering, Cornell University, Ithaca, NY, USA

Online publication date: 26 October 2010

**To cite this Article** Chen, Zhong and Escobedo, Fernando A.(2003) 'Simulation of Chain-length Partitioning in a Microfabricated Channel via Entropic Trapping', *Molecular Simulation*, 29: 6, 417 — 425

**To link to this Article:** DOI: 10.1080/0892702031000117117

**URL:** <http://dx.doi.org/10.1080/0892702031000117117>

PLEASE SCROLL DOWN FOR ARTICLE

Full terms and conditions of use: <http://www.informaworld.com/terms-and-conditions-of-access.pdf>

This article may be used for research, teaching and private study purposes. Any substantial or systematic reproduction, re-distribution, re-selling, loan or sub-licensing, systematic supply or distribution in any form to anyone is expressly forbidden.

The publisher does not give any warranty express or implied or make any representation that the contents will be complete or accurate or up to date. The accuracy of any instructions, formulae and drug doses should be independently verified with primary sources. The publisher shall not be liable for any loss, actions, claims, proceedings, demand or costs or damages whatsoever or howsoever caused arising directly or indirectly in connection with or arising out of the use of this material.

# Simulation of Chain-length Partitioning in a Microfabricated Channel via Entropic Trapping

ZHONG CHEN and FERNANDO A. ESCOBEDO\*

School of Chemical Engineering, Cornell University, 14850-5201, Ithaca, NY, USA

(Received October 2002; In final form January 2003)

A molecular simulation approach has been used to investigate the mechanism of entropic trapping for model linear DNA molecules as they go from a deep channel to a shallow channel driven by an electric field. In such a system, a molecule whose radius of gyration is larger than the gap of the shallow channel will tend to get temporarily trapped at its entrance. The free energy of the molecules as a function of chain position and the trapping times were obtained via Monte Carlo simulations. In weak to moderate electrical fields, the free energy barrier for escape  $\Delta F_{\text{max}}$  increases with chain length approaching a plateau value; in a strong electrical field,  $\Delta F_{\text{max}}$  exhibits a mild decreasing trend with chain length. At weak electric fields, shorter chains escape faster than longer chains because of their lower associated  $\Delta F_{\text{max}}$ . At moderate and strong fields, longer chains escape faster than shorter ones because, in the absence of significant differences in  $\Delta F_{\text{max}}$ , larger chains access a larger entrance area to the narrow channel; these results are in agreement with reported experimental observations. Preliminary results on the effect of chain branching on the escape rate are also presented.

**Keywords:** Entropic trapping; DNA partitioning; Molecular simulation; Monte Carlo

## INTRODUCTION

In recent years, the phenomenon of entropic trapping has received increasing amounts of attention in both theoretical and experimental investigations. Muthukumar and Baumgartner [1–3] have shown that a long polymer chain can be trapped entropically in an environment of randomly distributed pores of different sizes. In order to diffuse between the entropy-favorable larger open areas,

a chain molecule must squeeze through narrow passages that reduce its entropy. As a result, the dynamic process is slowed down significantly and the diffusion coefficient  $D$  exhibits a strong dependence on molecular size  $N$ . This effect is most prominent when the average size of the pores ( $\bar{a}$ ) is comparable to the radius of gyration ( $R_g$ ) of the polymer. Entropic trapping has also been observed experimentally as a new dynamic regime in gel electrophoresis [4]. Typically, the dynamics of polymers in gel-like media is described by the Rouse model (when  $R_g < \bar{a}$ ,  $D \sim 1/N$ ) and the reptation model (when  $R_g > \bar{a}$ ,  $D \sim 1/N^2$ ) [5,6]. However, the low-field diffusion coefficient was found to scale as  $D \sim 1/N^{2+\gamma}$  ( $\gamma > 0$ ) when  $R_g \approx \bar{a}$ , a result that is unaccounted for by standard models. The stronger dependence of  $D$  on  $N$  is a clear indication of the existence of entropic trapping. It appears that because pore sizes in the sieving gel are heterogeneous, polyelectrolytes such as DNA become entropically trapped in the larger pores. The value of parameter  $\gamma$  can be seen as a semiquantitative measure of the strength of the trapping effect, with  $\gamma = 0$  giving the reptation limit.

However, the random pore structure of polymer gels makes it difficult to attain a detailed microscopic understanding of the entropic trapping effect. Recently, new artificial entropic trapping devices have been constructed. For example, a microfabricated channel was developed by Han *et al.* [7–9] consisting of periodically alternating deep and shallow regions which was used to separate the components of a bidisperse solution of DNA molecules via electrophoresis. The  $R_g$  of the molecules being separated is smaller than the depth

\*Corresponding author. E-mail: escobedo@cheme.cornell.edu

of deep region, but it is larger than the depth of the shallow region. The DNA molecules can thus maintain their globular equilibrium shape in the deep region, but they must adopt a deformed “pancake”-like shape in the shallow region, at the cost of entropy loss. As a DNA molecule travels from the deep region to the thin region driven by an electrical field, it will be temporarily trapped at the entrance of the thin region before it can stretch its monomers into the thin region and form a beachhead for escape. This entropic trapping slows down the chain, whose mobility becomes now dependent on its length. Counterintuitively, for many of the conditions studied, longer DNA molecules were found to escape faster than shorter ones.

The well-controlled geometry used in the device described above facilitates the analysis and modeling of the entropic trapping effect. In an effort to understand the underlying mechanism, a simple kinetic model based on Transition State Theory (TST) was proposed in reference [7]. For a DNA molecule with some monomers already in the thin region, it was assumed that: (1) the increase of free energy due to the entropy loss is proportional to  $xT$ , where  $x$  is the length of DNA section in the thin region and  $T$  is the temperature; (2) the decrease of free energy due to the electrical field scales as  $x^2E_s$ , where  $E_s$  is the electrical field applied in the thin region. Therefore, the total free energy difference is  $\Delta F \sim xT - x^2E_s$  (which has a maximum of  $\Delta F_{\max} \sim 1/E_s$ ) and the trapping lifetime can be written as

$$\tau = \tau_0 \exp(\Delta F_{\max}/k_B T) = \tau_0 \exp(\alpha/E_s k_B T) \quad (1)$$

where  $\tau$  is the trapping lifetime,  $\Delta F_{\max}$  is the free energy barrier between the (incipient) trapped state and the transition state,  $k_B$  is the Boltzmann constant,  $\tau_0$  is a prefactor (a characteristic time constant), and  $\alpha$  is a constant. The experimental data of trapping times for different chain lengths and  $E_s$  values were consistent with a model wherein  $\Delta F_{\max}$  is independent of chain length. It was argued that DNA molecules overcome the barrier by stretching their monomers into the constriction, and once a proper length of beachhead is formed, the DNA molecule readily escapes the trap regardless of the molecular length still in the trap. The escape rate difference was explained by the fact that the surface area of a DNA molecule facing the slit is proportional to its coil diameter (i.e.  $\tau_0 \sim N^{-1/2}$  if the molecule satisfies Gaussian statistics). Even though this simple model was shown to be consistent with the experimental data, it is desirable to test the validity of each of the underlying model assumptions. Such assumptions are difficult to probe directly by experimental means, since this would require measuring the free energy landscape (that contains the barrier) along the “escape” coordinate.

In this work, we employed molecular simulation, which has been proven to be very useful in the study

of polymer chains under confinement environments, to investigate the thermodynamics and kinetics of a deep-shallow channel system. The simulation box adopted is similar (but not identical) to the geometry of the entropic trapping device used in experiment. Linear DNA was modeled as a flexible chain molecule consisting of a series of beads, where one bead represents one Kuhn segment. The electrical field inside the simulation box was calculated by solving Poisson–Laplace equation. The free energy as a function of chain position was obtained by the configurational-bias chain insertion method [10,11]. We used MC simulations with one-bead moves to generate sample trajectories of the molecular motion through the device and thus estimate escape rates ( $\tau^{-1}$ ). It was found that  $\Delta F_{\max}$  is a function of  $N$ ; for weak to moderate electrical field,  $\Delta F_{\max}$  increases with  $N$ , but  $\Delta F_{\max}$  becomes almost independent of  $N$  for large  $N$ . The escape rate decreases with  $N$  at weak  $E_s$  when  $\Delta F_{\max}$  is the dominating factor, but it increases with chain coil size over a certain range of  $N$  at larger  $E_s$  for which  $\Delta F_{\max} \sim k_B T$ . A few results are also presented for molecules with branched structure to elucidate the effect of chain architecture on escape rates.

## SIMULATION DETAILS

The system adopted for most of our simulations can be seen as a minimalistic, “generic” deep-shallow channel device (Fig. 1b). Although it was set up to capture some key features of the experimental system of Han *et al.* [7–9], several important simplifications and differences were introduced, namely: (1) Our system is reminiscent of one structure period of the experimental device but it is non-periodic (deep region has no entrance and shallow region is infinitely long), (2) the simulation process starts when the chain is in the deep region and the electric field is turned on (as opposed to a steady-state operation), (3) the channel physical dimensions are not identical to the experimental ones, (4) the inner device wall are assumed to be electrically neutral and (5) the interactions of DNA segments with one another, the solvent medium, the electric field, and the device walls are highly simplified. Details about these simplifications are given later in this section. Developing a more realistic model that better mimics experimental conditions is the object of ongoing efforts.

Linear DNA is coarse-grained as a flexible chain molecule consisting of a series of beads of uniform diameter  $\sigma$ , where one bead represents one Kuhn segment (for double-stranded DNA, one Kuhn segment contains about 340 bp and is approximately 100 nm in length [12,13]). The bond length is fixed at

$\sigma$  for free energy calculations, but is allowed to fluctuate within the range  $[\sigma - 0.15\sigma, \sigma + 0.15\sigma]$  for the escape rate simulations (described shortly). The simulations reported here refer to chains without excluded volume interactions (i.e. Gaussian chains). The chain lengths in our simulation range from  $N = 40$  to  $N = 320$  (radii of gyration in the bulk  $R_g^0$  range from 2.6 to  $7.4\sigma$  for Gaussian chains), which approximately correspond to double-stranded DNA molecules from 10 to 100 kbp. Typical DNA molecules used in experiment contain 5–200 kbp. One Kuhn segment of DNA molecule is assumed to carry  $-50e$  charges [14].

A diagram of the non-periodic simulation box is shown in Fig. 1b. The deep-region has a length of  $40\sigma$  ( $x$ -direction), and a “depth” of  $cl_z = 20\sigma$  ( $z$ -direction) which is comparable to (but larger than) twice the radius of gyration  $R_g$  of the model chains studied. The depth of the shallow region is  $D_s = 3\sigma$ , which is much smaller than  $2R_g$ . The box extends infinitely in the  $y$  direction. Hard-wall repulsive interactions are exerted when the center of a bead approaches the boundaries of the box in the  $x$  and  $z$ -directions. In all the free energy calculations and in most of the escape simulations, no periodic

boundary conditions (PBC) are applied in the  $x$ -direction; instead, a hard wall closes the entrance to the deep region and the channel is extended infinitely in the shallow region. Note that in the experiments [7], the  $x$ -length of the shallow region is usually much longer than the stretched chain coil; therefore, a chain that partially penetrates the thin region does not get near the entrance to the next deep region. For comparison, a few escape simulations were performed for a system with PBC in the  $x$ -direction (Fig. 1a) and with a shallow-region length of  $40\sigma$ .

The electrical field in the simulation box is obtained by numerically solving Poisson–Laplace equation

$$\frac{\partial^2 \phi}{\partial x^2} + \frac{\partial^2 \phi}{\partial z^2} = 0$$

where  $\phi$  is the electrical potential. Dirichlet boundary conditions are applied at  $x = -0.5cl_x$  (for the entire plane in Fig. 1b but only for the thin-channel opening in the case of PBC in the  $x$ -direction) and at  $x = +0.5cl_x$ , where  $\phi = 0$  and  $\phi_s$ , respectively. Neumann boundary conditions (i.e.  $\partial\phi/\partial x = 0$  or  $\partial\phi/\partial z = 0$ ) are applied at the other walls, under

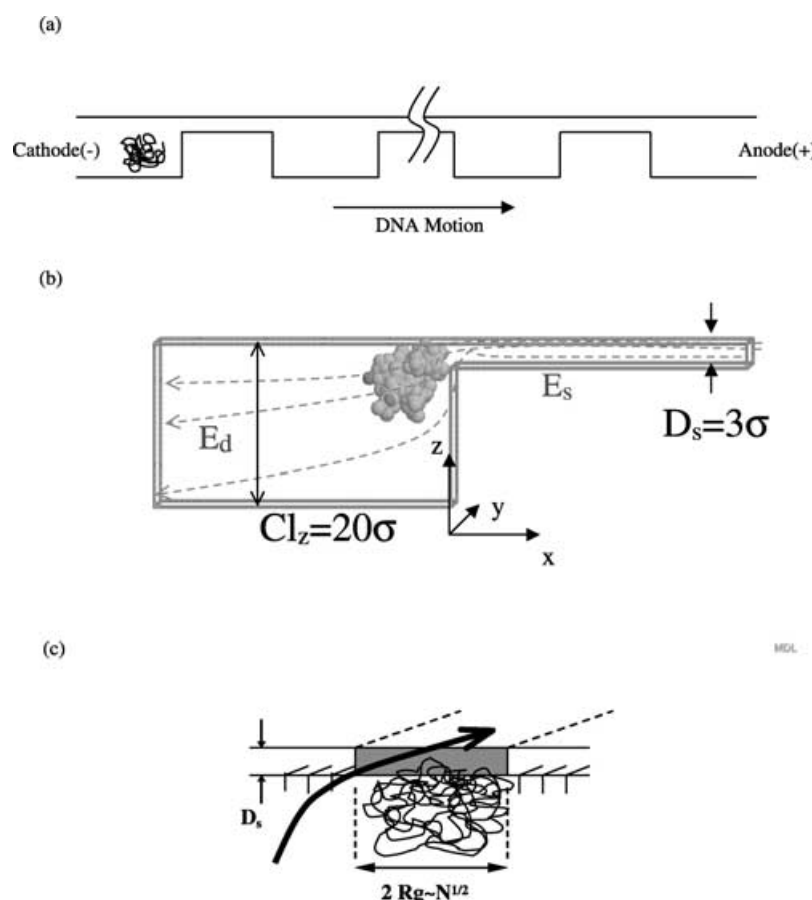


FIGURE 1 (a) Schematic diagram of experimental device used in Ref. [7]. (b) The simulation box without PBC in the  $x$ -direction. (c) A cartoon of a DNA molecule at the entrance to the shallow region as seen along the  $x$ -direction. The system in (a) can be mimicked by a simulation box with PBC in the  $x$ -direction.



the assumption that they are electrically neutral. Note, however, that in experiments the Si channels are covered by a Pyrex coverslip which does become charged when in contact with an electrolyte solution. While this surface charge will affect the electrical field inside the channel and sustain electroosmotic flow, such effects have been argued to play a minor role in the entropic trapping process [7] and have thus been neglected here. The strength of the electrical field is characterized by its value  $E_s$  in the thin channel and the value of  $\phi_s$  is set to  $0.5\text{cl}_x(E_s + E_d)$  under the assumption that the electrical fields are uniform in the thin region ( $E_s$ ) and the deep region ( $E_d$ ). Apparently,  $E_d = \frac{D_s}{\text{cl}_x} E_s$ . The electrical field at every point was obtained numerically by a finite difference method, i.e.  $E_x = -\Delta\phi/\Delta x$ , and  $E_y = -\Delta\phi/\Delta y$ . Our results show that except for field gradients near the box edges at the entrance to the thin channel, the electrical fields are indeed almost uniform and aligned parallel to the  $x$  axis. However, our Monte Carlo simulations show that the converging electrical field at the entrance of the shallow region is very important for the escape of trapped molecules (results not shown). The input values of  $E_s$  are varied to simulate different strengths of the electrical field. In order to observe entropic trapping effects, fields of intermediate strength should be chosen in such a way that  $\Delta F_{\text{max}} \sim k_B T$ . The value of  $E_s$  reported in this paper has been reduced by  $k_B T/e\sigma$ , where  $e$  is the electron charge.

### Free Energy Calculations

The changes of the molecular free energy ( $F$ ) along the escape path describe the underlying thermodynamic driving force for chain escaping. In particular, the free energy barrier height  $\Delta F_{\text{max}}$  of such landscape is used by transition state theory to quantify escape rates. In this work, the excess free energy as a function of the chain position is obtained by using the chain insertion method with configurational-bias sampling [10,11]. The first bead is placed with uniform probability along the  $x$ -direction. The whole chain is then grown bead by bead in a configurational-bias fashion. The Rosenbluth weight for the insertion of the  $i$ th segment is

$$w_i = \frac{\sum_{j=1}^k \exp[-\beta u(j)]}{k}$$

where  $k$  is the total number of trial positions,  $\beta = 1/k_B T$ , and  $u(j)$  is the energy associated with the  $j$ th trial position. Among these  $k$  trial positions, one is chosen in a way that favors the largest Boltzmann factor. We adjust the value of  $k$  to be large enough so that almost every insertion attempt can be completed (less than one failed out of a million attempts). The excess free energy of the whole chain (with reference

to a free chain) is given by

$$\beta\Delta F_{x^*} = -\ln \left\langle \prod_{i=1}^N w_i \right\rangle_{x^*}$$

where the average is over all completed attempts at a certain position  $x^*$ . The  $x^*$  position provides the "escape" coordinate to monitor the DNA journey from the deep region to the narrow region.

### Escape Simulations

The existence of the free energy barrier along the escape path implies that the molecule spends most of its journey time at the narrow channel entrance changing conformations and slowly stretching into the narrow channel. In such a state, the molecule as a whole experiences little overall translation and relaxational dynamics becomes the dominant mechanism for conformational changes. In these simulations, molecular rearrangements were performed via "dynamic" Monte Carlo moves, namely, hop and flip moves. In a hop move, a bead displacement is attempted in a random direction and by a random distance. In a flip move, a bead rotation is attempted by a random angle around the line connecting the centers of the two neighbor beads. A proposed move is accepted according to the Metropolis criterion. This type of dynamic Monte Carlo is known to be able to produce chain dynamics according to the Rouse model [15] (e.g. diffusive motion). Of course, the motion of a long polymer chain in such a system can be more accurately described by models that include hydrodynamic interactions between beads, such as the Zimm model [16], and hydrodynamic interactions between the beads and the walls. Nonetheless, Rouse dynamics is one of the dominant modes for chain relaxation dynamics in the trapped state (perhaps the most dominant) and thus constitutes a good starting point for future investigations.

The trapping time  $\tau$  of DNA molecule is "measured" in units of MC cycles. In every MC cycle, each bead moves in average once (via hop and flip moves). In simulations without PBC in the  $x$ -direction, the initial configuration is generated randomly in the deep region and relaxed for  $5 \times 10^5$  cycles with the electrical field turned off. The simulated escape process thus always begins from a fully relaxed configuration. Note that this does not corresponds to what happens in experimental devices with short period length, where the DNA molecule may not have enough time to relax in the deep region before it reaches the entrance to the thin region (such an arrested relaxation can have an important effect on  $\tau$ ).  $\tau$  is defined as the time elapsed from the moment the electrical field is turned on to the moment when the center of mass of the chain

passes the  $x = 40\sigma$  plane. For any particular chain length and electric field, between 50 and 100 escape trajectories were generated to obtain good statistics for the average  $\tau$ . For simulations with PBC in the  $x$ -direction, the simulation begins with the chain randomly placed in the deep region, and then follows the chain trajectory as it crosses the traps, one after another through the periodic boundary. The value of  $\tau$  is averaged over a prescribed number (50–100) of deep-narrow passages in one run.

## SIMULATION RESULTS

### (a) Free Energy Barrier

When part of the DNA molecule changes conformation to stretch into the thin channel, the entropy loss associated with this deformation leads to an increase in free energy. At the same time, as DNA monomers move along the direction of the electrical-field force, the total energy is reduced which decreases the free energy of the whole chain. At appropriate conditions, the interplay between those two competing effects will result in a maximum in free energy  $F$  along the escape path, which can be identified as the transition state for TST.

The free energy barrier for escape  $\Delta F_{\max}$  can be readily found if the values of excess free energy  $F$  are plotted against chain position  $x^*$  (i.e. the reaction coordinate in TST), and the transition state is identified. There are several possible choices for the reaction coordinate, such as the number of sites in the shallow region, the maximum penetration distance into the shallow region, the center of mass (COM) of the chain in the  $x$ -direction, and the degree of penetration. The degree of penetration is defined as  $\sum_{i=1}^{N_s} x_i/N$ , where  $N_s$  is the number of beads in the thin channel, and  $x$  is the penetration distance into the thin region. A good choice for the reaction coordinate is one that has a clear physical meaning and gives a distinct location of the transition state. Our simulation results suggest that the degree of penetration is the best choice among all the choices mentioned above. Sample curves are shown in Fig. 2, where the free energy at  $E_s = 2.5 \times 10^{-4}$  is plotted against both the COM position and the degree of penetration. When plotted against the COM position, the free energy increases as the chain approaches the entrance to the thin region and stays relatively flat until the COM of the chain is well into the thin region. However, when plotted against the degree of penetration, the free energy curve exhibits one well-defined maximum, which can be conveniently defined as the transition state for our analysis. For the ensuing discussions then, the degree of penetration is chosen as the escape coordinate.

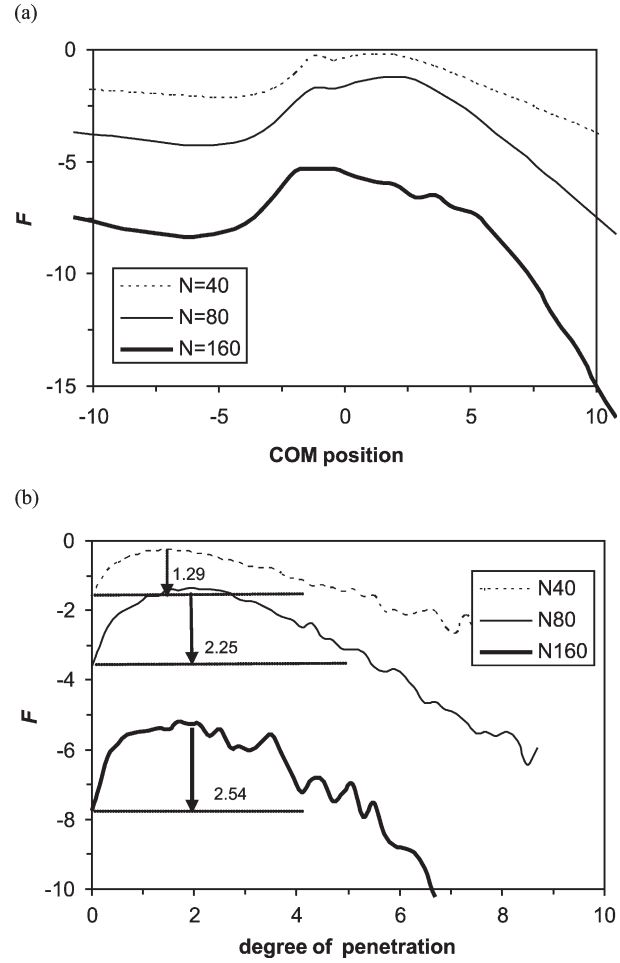


FIGURE 2 Free energy  $F$  at  $E_s = 2.5 \times 10^{-4}$  as function of (a) the center of mass position in the  $x$ -direction and (b) the degree of penetration.  $F$  is in units of  $k_B T$ .

As shown in Fig. 2(b), the free energy barrier  $\Delta F_{\max}$  increases with chain length, which can be explained by the larger entropy loss that occurs when a larger chain is confined into a narrow slit. It is well known that the free energy increase of a Gaussian chain due to confinement in a narrow slit grows linearly with  $N$  [17]. Interestingly, the degree of penetration at the transition state is almost the same for chains with  $N = 80$  and  $160$ , which suggests that more chain segments inside the shallow region are required to force a larger chain past the barrier. Figure 3 shows  $F$  as a function of the degree of penetration at  $E_s = 3.75 \times 10^{-4}$ . Compared to Fig. 2(b), it is observed in Fig. 3 that: (1)  $\Delta F_{\max}$  decreases as the electrical field is intensified;  $\Delta F_{\max} > k_B T$  for  $E_s = 2.5 \times 10^{-4}$  (a weak electrical field), while  $\Delta F_{\max} < k_B T$  for  $E_s = 3.75 \times 10^{-4}$  (a moderate electrical field), (2) the trend of increasing  $\Delta F_{\max}$  with  $N$  is still observed, but the difference between the longer chains ( $N = 80$  and  $160$ ) is negligible and (3) for the same chain length, the degree of penetration at the transition state (i.e. at the maximum in the curve) decreases with increasing  $E_s$ . The relation between

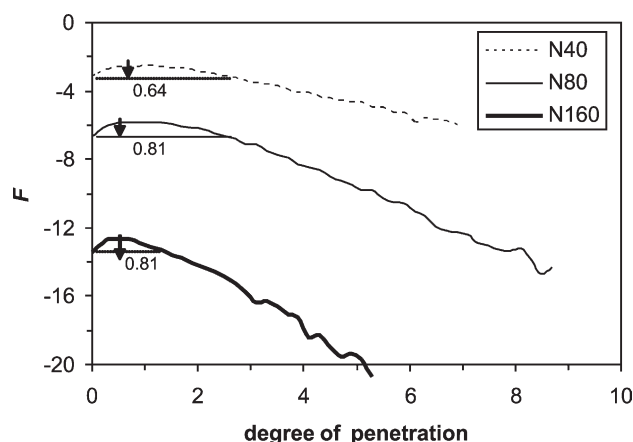
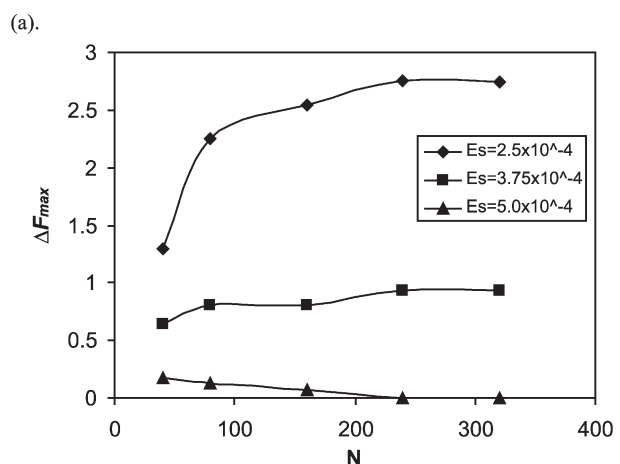


FIGURE 3 Free energy  $F$  as a function of the degree of penetration at  $E_s = 3.75 \times 10^{-4}$ .

$\Delta F_{\max}$  and  $N$  for different electrical fields can be seen more clearly in Fig. 4(a). At weak and moderate field, there is a steep increase in  $\Delta F_{\max}$  as the chain length increases from  $N = 40$  to  $80$ ; however, from  $N = 80$  to  $320$ ,  $\Delta F_{\max}$  increases at a steady but much slower rate ( $< 20\%$ ). Systems with  $E_s = 5.0 \times 10^{-4}$  and  $7.5 \times 10^{-4}$  appear to correspond to strong field scenarios since  $\Delta F_{\max}$  approaches zero for all chain lengths.

### (b) Escape Simulations

Figure 4(b) shows the trapping time  $\tau$  as a function of chain length at different electrical fields. At weak electrical field ( $E_s = 2.5 \times 10^{-4}$ ),  $\tau$  increases with chain length, which correlates with the associated increase in  $\Delta F_{\max}$  [shown in Fig. 4(a)]. At strong electrical field (e.g.  $E_s = 5.0 \times 10^{-4}$  and  $7.5 \times 10^{-4}$ ), however,  $\tau$  decreases with chain length. At strong  $E_s$ ,  $\Delta F_{\max}$  is small for all chain lengths and the prefactor  $\tau_0$  in Eq. (1) becomes dominant; since longer chains have larger access surface area to the thin channel entrance (smaller  $\tau_0$ ), they escape faster. As the chain size approaches 240, the escape time curve levels off and seems to reach a plateau. At moderate electrical field ( $E_s = 3.75 \times 10^{-4}$ ), there is a maximum in  $\tau$  for  $N = 80$ , resulting from the interplay between the free energy factor [ $\exp(\Delta F_{\max}/k_B T)$ ] and chain size factor ( $\tau_0$ ). From  $N = 40$  to  $80$ , there is a substantial increase in  $\Delta F_{\max}$  [see Fig. 4(a)], which slows the escaping process more than what the decrease in  $\tau_0$  can make up for. For chains longer than  $N = 80$ ,  $\tau$  decreases with  $N$ , following a trend similar to that observed at strong field. However, the differential trapping time  $-d\tau/dN$  (i.e. the selectivity of the entropic trapping device) increases as the electrical field is varied from strong to moderate strength. Therefore, moderate electrical fields (i.e.  $\Delta F_{\max} \sim k_B T$ ) are best for DNA separation, which is consistent with experimental observations [7]. In a moderate electric field,



(b).

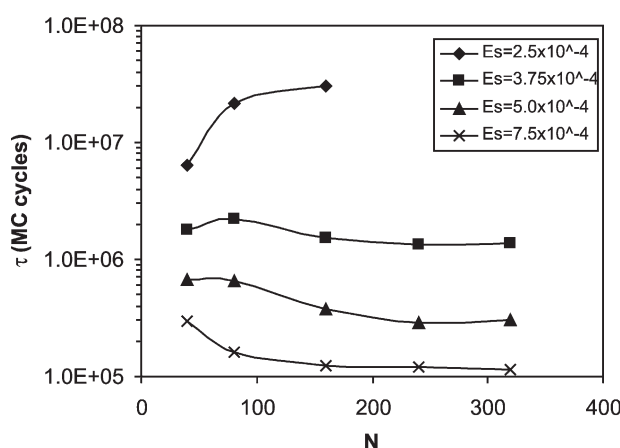


FIGURE 4 (a) Escape free energy barrier  $\Delta F = \Delta F_{\max}$  and (b) trapping time as a function of chain length at different electrical fields.

DNA molecules still have good mobility while the selectivity is much better than in a strong field. Similar results were also observed for chains with excluded volume interactions (results not shown).

Since conformational changes of the chain molecule at different stages of the escaping process correlate with entropy loss, a detailed analysis of such changes along the escape path may reveal important information on the entropic trapping mechanism. For this purpose, the mean-squared radius of gyration  $R_g^2$  and its components in the  $x$ ,  $y$  and  $z$ -directions [ $R_g^2(x)$ ,  $R_g^2(y)$  and  $R_g^2(z)$ , respectively] were calculated in the escape simulations for different positions of the chain COM. The results for a molecule with  $N = 80$  at  $E_s = 3.75 \times 10^{-4}$  are shown in Fig. 5. As the DNA chain moves along the escape path,  $R_g(y)$  remains essentially unchanged while  $R_g(z)$  decreases from its unperturbed size to a value  $< D_s/2$ ; the deformation in the  $x$ -direction is the least trivial and appears to determine the overall

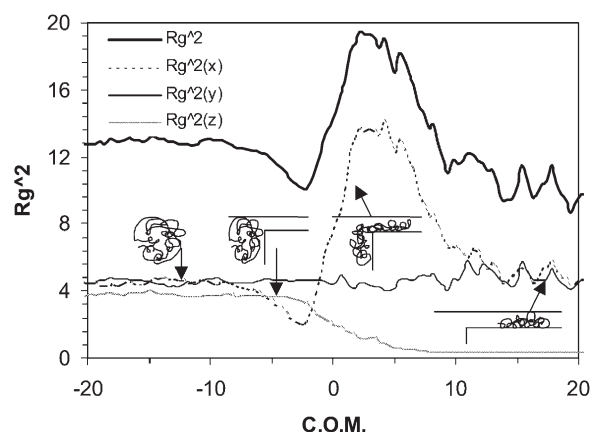


FIGURE 5 Mean-squared radius of gyration  $R_g^2$  and its three components in the  $x$ ,  $y$  and  $z$ -directions as a function of the center of mass (COM) position for a model chain with  $N = 80$  during escape simulations at  $E_s = 3.75 \times 10^{-4}$ . Four chain conformations at different positions are also schematically depicted, from left to right: unperturbed, compressed, stretched and recoiled.

shape of the molecule [as seen in the shape similarity between the  $R_g^2$  and  $R_g^2(x)$  curves]. When the molecule approaches the entrance to the thin region, its movement along the  $x$ -direction is hindered by the wall and the coil tends to be compressed by the electrical force, leading to a decrease in  $R_g^2$  and  $R_g^2(x)$ . At that point, some of the monomers begin to penetrate into the thin region via localized rearrangements. Once some parts of the chain get inside the thin region, they will be stretched in the  $x$ -direction by the stronger local electrical field, and eventually increase  $R_g^2(x)$  and lead to the upturn in the curve. The position where  $R_g^2$  and  $R_g^2(x)$  have minimum values signals the transition state in the escape path. After the chain passes the transition state, more and more chain segments are pulled into the thin region and are stretched in the  $x$ -direction, increasing  $R_g^2$  and  $R_g^2(x)$ . This increasing trend continues until the whole chain is in the thin region. At that point, the chain begins to relax in a confined nearly two-dimensional environment and recoils back in the  $x$ -direction so that  $R_g^2(x)$  approaches  $R_g^2(y)$ . Note that the constancy of  $R_g^2(y) \sim R_g^2/3$  supports the idea that in evaluating the relation between  $\tau_0$  and the entrance “window” area [of dimensions  $D_s \times 2R_g(y)$ ] accessible to a DNA molecule, one is justified to use  $\tau_0 \propto R_g^{-1} \propto N^{-1/2}$ .

We also investigated the effect of branching on  $\tau$ . For this purpose, the escape times of 3-arm star molecules with different molecular weight ( $N = 82, 160, 241$  and  $322$ , respectively) were simulated. The results for  $E_s = 5.0 \times 10^{-4}$  are reported in Fig. 6 where  $\tau$  is plotted against  $R_g^0$ ; data for linear chains from  $N = 80$  to  $320$  are also plotted for reference. The escape time for star molecules decreases with  $N$ , following a trend similar to that of linear chains. It is observed that within simulation uncertainties, the data points for star and linear molecules collapse

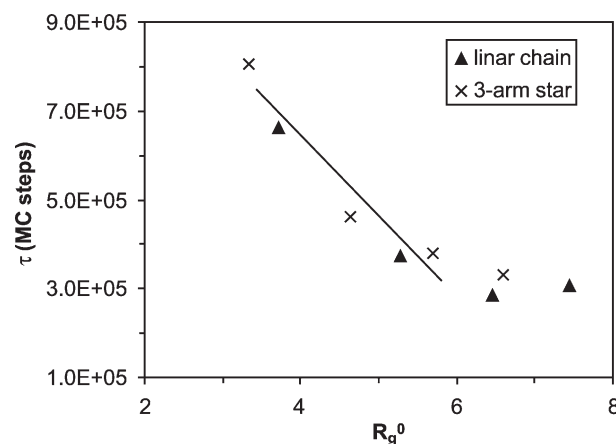


FIGURE 6 Trapping time as a function of  $R_g^0$  at  $E_s = 5.0 \times 10^{-4}$  for linear chains and 3-arm stars. Solid line (drawn to guide the eye) shows a linear correlation.

onto a single curve. This suggests that in that range of chain lengths, coil size (e.g.  $R_g$ ) as opposed to molecular weight ( $N$ ) is the determinant factor of trapping times, while chain topology (i.e. branching pattern) only plays a minor role. In particular, a nearly linear correlation between escape time and  $R_g^0$  can be found between  $N = 80$  and  $160$ , as shown by the straight line.

All the simulations discussed so far were performed without PBC in the  $x$ -direction, beginning from a relaxed chain configuration. It is expected that the state of relaxation of the initial chain conformation will have some effect on the time spent to move across the straight regions, but little effect on the time needed to get across the constriction (for a sufficiently long deep-region). To test this conjecture, we also conducted a few simulations in a device with PBC in the  $x$ -direction (that more closely approaches the operation of the reported experimental device, Fig. 1a). Figure 7 shows the results for the “net” trapping time for systems with and without PBC in the  $x$ -direction for chain with  $N = 160$ . Here, the “net” trapping time  $\tau'$  is the time elapsed from the moment when the first chain-site crosses into the shallow region (even if it comes back out again) to the moment when the last chain-site leaves the deep region. Because the electrical field inside the simulation box depends on the boundary conditions employed, an effective  $E'_s$  for the transition region was used in Fig. 7 that corresponds to the difference of electrical potential between the middle  $x$ -positions of the deep and the shallow channels. A linear correlation is observed between  $\log(\tau')$  and  $1/E'_s$ , consistent with Eq. (1). The results with and without PBC collapse onto the same curve, which supports the conjecture that the initial configuration has little effect on the barrier-crossing time (at least for this set of conditions).



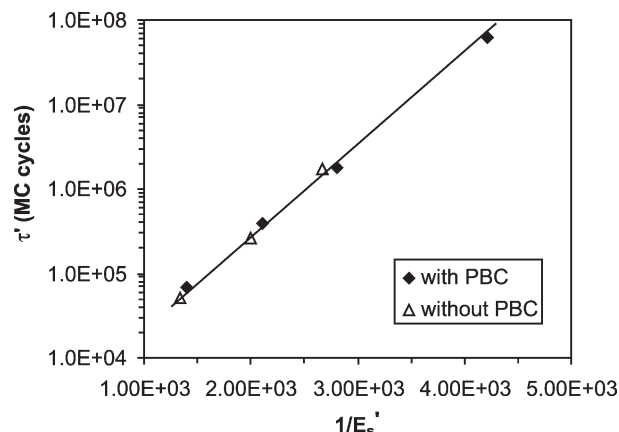


FIGURE 7 Comparison of net trapping times from simulations with and without PBC in the  $x$ -direction for a chain with  $N = 160$ . The logarithm of trapping time is plotted against  $1/E_s'$ , where  $E_s'$  is the effective electrical field based on the potential difference across the barrier. A linear trend is observed, as shown by the straight line.

## CONCLUDING REMARKS

In this paper, the mechanism of entropic trapping of linear DNA molecules going through a non-periodic, regular-shaped constriction was investigated using molecular simulations. The simulations probed the thermodynamics (free energy landscape) and the kinetics (escape times) of entropic trapping. The free energy of linear chains was obtained via configurational-biased chain insertion method for varying chain position, chain length and electrical field strength. It was found that when the degree of penetration is chosen as the “escape” path, there is a well-defined maximum in the free energy curve that allows the estimation of the free energy barrier  $\Delta F_{\max}$ . At weak and moderate electrical fields,  $\Delta F_{\max}$  is shown to increase with  $N$ , but this increase is only significant for short chains (e.g. from  $N = 40$  to  $80$ ) and is almost negligible for longer chains. At strong electrical field, however,  $\Delta F_{\max}$  decreases with  $N$ . The trapping time was simulated using a “dynamic” Monte Carlo approach at different electrical field conditions, ranging from weak to strong fields. At weak electrical field, it was found that the trapping time increases with increasing  $N$ , suggesting that the free energy barrier term  $\exp(\Delta F_{\max}/k_B T)$  is the controlling factor in the escaping process. At moderate to strong electrical field, the trapping time decreases with  $N$ , suggesting that the prefactor  $\tau_0$  (which decreases with chain coil diameter) is the controlling factor in the process. Test simulations performed for a periodic system (mimicking a series of deep-narrow passages) showed that the net trapping time (needed to cross the barrier) is little sensitive to the initial relaxation state of the chain in the deep region.

It was observed that to achieve optimal partitioning between DNA molecules of different chain lengths, the electrical field should be chosen in such a way that the escape free energy barrier is of the order of  $k_B T$ . At such conditions, DNA molecules have enough mobility to cross the barrier relatively fast and yet substantial differences exist in the escape rates of chains of different lengths. The conjecture (based on experimental data) that the height of the free energy barrier is the same regardless of chain length was found to be approximately true for long chains at moderate to strong electrical fields. Because our simulations spanned a range of conditions that fully probed the interplay between the free-energy barrier factor  $\exp(\Delta F_{\max}/k_B T)$  and the chain size factor  $\tau_0$ , the escape rate exhibited a more complicated pattern of behavior than in experiment. Furthermore, a general “scaling” formulation for the free energy difference as a function of penetration distance [7] appears to be an oversimplification given that the chain sections that first penetrate the thin region adopt irregular and stretched conformations.

There are several aspects in our simulations that can be improved. The depth of the thin region is 90 nm in the experimental system, which is commensurate to the Kuhn segment length of a DNA molecule. In our simulations,  $D_s$  was increased to three Kuhn lengths to give the molecule enough conformational freedom to penetrate the narrow region (the molecule is unlikely to penetrate a slit where it would become a 2-dimensional object). In order to mimic more closely the experimental conditions, one Kuhn segment should be represented by several beads with semi-flexible bond–bond angles so that the model DNA molecule becomes deformable at a small enough length scale to be able to squeeze into a one-Kuhn-length deep channel. In mapping out the free-energy landscape, complementary calculations of the chain chemical potential should be performed (using alternative methods) since it is known that configurational-bias insertion techniques can produce non-representative conformations for long chains. The effects of a charged upper plate (if made of glass) and of the extent of chain relaxation in the deep region should be investigated in detail as they may significantly enhance or retard the separation effect. As indicated earlier, the dynamic Monte Carlo method employed in the escape simulations can only reproduce properties from purely diffusional relaxation dynamics. Even though the neglect of hydrodynamic effects in the systems studied could be permissible under some conditions, Brownian Dynamics simulations with proper account for hydrodynamic effects will certainly provide a more realistic description of the process. Efforts along all those directions are currently underway.

### Acknowledgements

This work was supported by the U.S.A. Department of Energy, DE-FG02-02ER15291.

### References

- [1] Baumgärtner, A. and Muthukumar, M. (1987) "A trapped polymer chain in random porous media", *J. Chem. Phys.* **87**, 3082.
- [2] Muthukumar, M. and Baumgärtner, A. (1989) "Effects of entropic barriers on polymer dynamics", *Macromolecules* **22**, 1937.
- [3] Muthukumar, M. and Baumgärtner, A. (1989) "Diffusion of a polymer chain in random media", *Macromolecules* **22**, 1941.
- [4] Arvanitidou, E. and Hoagland, D. (1991) "Chain-length dependence of the electrophoretic mobility in random gels", *Phys. Rev. Lett.* **67**, 1464.
- [5] de Gennes, P.-G. (1979) *Scaling Concepts in Polymer Physics* (Cornell University Press, Ithaca, NY).
- [6] Doi, M. and Edwards, S.F. (1986) *The Theory of Polymer Dynamics* (Clarendon Press, Oxford).
- [7] Han, J., Turner, S.W. and Craighead, H.G. (1999) "Entropic trapping and escape of long DNA molecules at submicron size constriction", *Phys. Rev. Lett.* **83**, 1688.
- [8] Han, J. and Craighead, H.G. (2000) "Separation of long DNA molecules in a microfabricated entropic trap array", *Science* **288**, 1026.
- [9] Han, J. and Craighead, H.G. (2002) "Characterization and optimization of an entropic trap for DNA separation", *Anal. Chem.* **74**, 394.
- [10] de Pablo, J.J., Laso, M. and Suter, U.W. (1992) "Estimation of the chemical potential of chain molecules by simulation", *J. Chem. Phys.* **96**, 2395.
- [11] Frenkel, D. and Smit, B. (2002) *Understanding Molecular Simulation: From Algorithms to Applications*, 2nd Ed. (Academic Press, New York).
- [12] Post, C.B. (1983) "Excluded volume of an intermediate-molecular-weight DNA—a Monte-Carlo analysis", *Biopolymers* **22**, 1087.
- [13] Hagerman, P.J. (1988) "Flexibility of DNA", *Annu. Rev. Biophys. Biophys. Chem.* **17**, 265.
- [14] Smith, S.B. and Bendich, A.J. (1990) "Electrophoretic charge-density and persistence length of DNA as measured by fluorescence microscopy", *Biopolymers* **29**, 1167.
- [15] Bilchev, A. and Binder, K. (1997) "Dewetting of thin polymer films adsorbed on solid substrates: a Monte Carlo simulation of the early stages", *J. Chem. Phys.* **106**, 1978.
- [16] Zimm, B.H. (1956) "Dynamics of polymer molecules in dilute solution—viscoelasticity, flow birefringence and dielectric loss", *J. Chem. Phys.* **24**, 269.
- [17] Gorbunov, A.A. and Skvortsov, A.M. (1995) "Statistical properties of confined macromolecules", *Adv. Colloid Interface Sci.* **62**, 31.